RSC Advances

This is an *Accepted Manuscript*, which has been through the Royal Society of Chemistry peer review process and has been accepted for publication.

Accepted Manuscripts are published online shortly after acceptance, before technical editing, formatting and proof reading. Using this free service, authors can make their results available to the community, in citable form, before we publish the edited article. This *Accepted Manuscript* will be replaced by the edited, formatted and paginated article as soon as this is available.

You can find more information about *Accepted Manuscripts* in the Information for Authors.

Please note that technical editing may introduce minor changes to the text and/or graphics, which may alter content. The journal's standard Terms & Conditions and the Ethical guidelines still apply. In no event shall the Royal Society of Chemistry be held responsible for any errors or omissions in this *Accepted Manuscript* or any consequences arising from the use of any information it contains.

ROYAL SOCIETY OF CHEMISTRY

www.rsc.org/advances

Journal Name

RSCPublishing

COMMUNICATION

Improving photocurrent of PBDTTT-CF and PCBM based organic thin film photoconductor by forming bilayer structure

Zhiwen Jin[1], *Qing Zhou*[1], Peng Mao[1], *Aiji Wang*[2], *Boyang Shang*[2], *Yinshu Wang*[2], *Hui Li*[1]* and *Jizheng Wang*[1]*

Cite this: DOI: 10.1039/x0xx00000x

Received 00th January 2012,
Accepted 00th January 2012

DOI: 10.1039/x0xx00000x

www.rsc.org/

Performance of traditional organic thin film photoconductors (OTFPs) is limited by the low carrier mobility in the donor:acceptor (D:A) blend film. To overcome such a problem, higher-mobility carrier transport layer should be brought in the D:A blend based device. However doing so will certainly result in bilayer or even multilayer structure, which is usually a challenge for all-solution processing methods. Here by carefully controlling and adjusting the fabrication process, all-solution-processed PBDTTT-CF/PBDTTT-CF:PCBM bilayer OTFP is demonstrated. In such a bilayer device, PBDTTT-CF:PCBM blend layer is responsible for light absorption and free photo carrier generation, and the underlying PBDTTT-CF layer is responsible for the photo carrier transportation inside the device. The hole mobility in the PBDTTT-CF layer is measured to be 9.1×10^{-4} $cm^2V^{-1}s^{-1}$, much higher than that in the PBDTTT-CF:PCBM blend film, which is only 4.3×10^{-5} $cm^2V^{-1}s^{-1}$. As a result of the faster carrier transport, the bilayer device exhibits a greatly enhanced photocurrent, which is about 7 times higher than that of the single blend layer device. Meanwhile, the ON/OFF response of the bilayer device is also improved, which is shorter than 0.1/0.1 s.

1. Introduction

Due to their great virtues of low-cost fabrication and high flexibility, organic thin film photoconductors (OTFPs) are expected to have broad applications in the field of optical communications, artificial vision and biomedical sensing.[1-6] Tremendous efforts have been made in developing OTFPs with donor:acceptor (D:A) blend active layers: Jeong et al.[7] firstly brought donor:acceptor blend into OTFPs to enhance the generation of photo carriers.[8,9,10]); Followed, Peet et al.[11] further enhanced the performance of OTFPs by adding additive in the D:A blend film, which is able to improve nano-morphology of the blend film and hence benefit free carrier generation; Later, [70]PCBM (analogue of PCBM and displays improved light absorption[12]) is used in the blend film to enlarge light absorption, and higher photocurrent was obtained;[13] Recently, Li et al.[14] successfully further improved the performance of the OTFPs using a substrate with patterned photonic crystals which is capable of increasing the reflection light and hence the overall light absorption of the blend film. Although these progresses are encouraging, the performance of OTFPs remains unsatisfactory. Careful analysis can find that above studies mainly concentrated on increasing the numbers of photo carriers with a blend layer responsible not only for carrier generation but also for carrier transport. The organic blend film is of course sufficient for light absorption and carrier generation,[15] but the nanoscale network formed in the blend film greatly increases the distance carrier travels between the two electrodes, and hence seriously weakens carrier mobility and slows down carrier transport inside the device.[16-19] A feasible approach to solve this problem could be: layer with higher carrier mobility be brought in to transport photo carriers generated in the low-mobility D:A blend film.

In this paper, by an all-solution processing method bilayer OTFPs are fabricated: a D:A blend layer of PBDTTT-CF:PCBM for carrier generation (PCBM:[6,6]-phenyl-C61-butyric acid ethyl ester, PBDTTT-CF: poly[4,8-bis-substituted-benzo[1,2-b:4,5-b']dithiophene-2,6-diyl-alt-4-substituted-thieno [3,4-b] thiophene-2,6-diyl]-fluorine, hereafter referred as CF), and a layer of CF for carrier transport. Due to the much higher carrier mobility in the CF film (in comparison to that in the CF:PCBM blend film), the bilayer device exhibits a ~7 times higher photocurrent than that of the traditional single layer device with only CF:PCBM blend layer. The bilayer device presents a R value of 1.3 AW^{-1}, significantly higher than that 0.19 AW^{-1} of the traditional blend-only device.

RSC Advances Accepted Manuscript

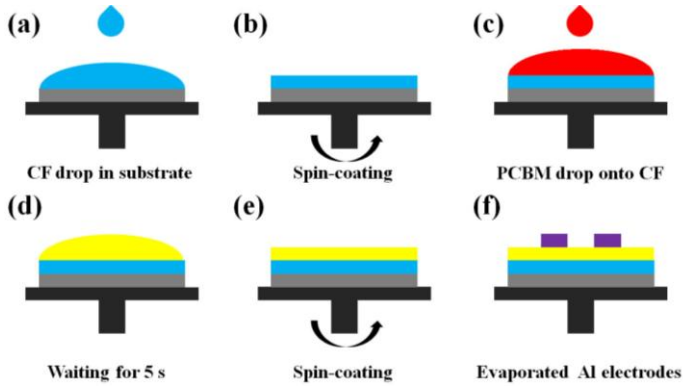

Figure 1. Fabrication of the bilayer photoconductor.

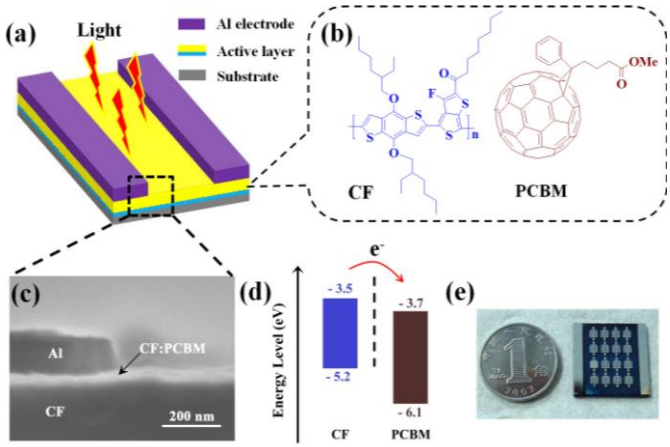

Figure 2. (a) Schematic illustration of the bilayer OTFPs. (b) The molecular structures of CF and PCBM. (c) The cross-sectional SEM image of the fabricated bilayer device. (d) Energy band diagram of CF and PCBM. (e) The photograph of the fabricated device.

2. Experimental Section

2.1 Materials and Substrates

All of the materials were purchased from Sigma-Aldrich and were used as received without further purification. The Corning Eagle XG glasses and N-doped silicon with 300 nm silicon dioxide were used as the substrates for the photoconductors and field effect transistors.

2.2 Solution Ratio and Concentration

The concentration of the CF solution and the blend solution (CF:PCBM ratio of 1:1.5) in o-dichlorobenzene were 40 mg/ml. The concentration of the PCBM solution in dichloromethane (DCM) was 10 mg/ml. The solutions were stirred rigorously for ca. 24 h at room temperature.

2.3 Device Fabrications

The CF film, the PCBM film and the CF:PCBM blend film were formed by spin-coating their solutions onto the substrate at 1000 rpm for 30 seconds. The step-by-step fabrication process of the bilayer film is shown in **Figure 1**: (a) CF solution was dropped onto the substrate; (b) the CF film was subsequently formed after spin-coating; (c) PCBM solution in DCM was dropped onto the prepared CF film; (d) 5s wait: owing to the high solubility of PCBM in DCM[20,21] and extremely poor solubility and hence slow dissolution rate of CF in DCM (proved by the experiments), only a small amount of the CF on top of the CF film was dissolved into PCBM drop by DCM, converting the pure PCBM drop into CF:PCBM blend drop; (e) after spin-coating, the blend layer is formed, and so is the bilayer structure; (f) the device was completed with thermal evaporation of 100 nm-thick Al electrodes through a shadow copper grid mask, which results in a channel width of 2000 μm and a channel length of 10 μm.

It should be noted that the OTFPs (for the CF film, the PCBM film, the CF:PCBM blend film and the bilayer film) were fabricated on glass substrates while the organic thin film transistors (OTFTs) (for the CF film, the PCBM film, and the CF:PCBM blend film) were fabricated directly on the SiO_2 (300 nm)/Si^+ substrate (for testing the hole mobility in CF based TFT, Au electrodes instead of Al electrodes were used).

2.4 Measurements

Electrical characterizations were recorded with a Keithley 4200 and a Micromanipulator 6150 probe station at room temperature. A white-light halogen–tungsten lamp with power intensity of 1.5 $mWcm^{-2}$ was used for illumination. The light intensity was calibrated using a mono-silicon detector produced by the National Renewable Energy Laboratory (NREL). The monochromatic light is from a Newport Oriel 200^{TM}, and the intensity is 10.6 $\mu W/cm^2$. Prior to the use of monochromatic light, the spectral response of the mono-silicon solar cell was measured and normalized to the NREL standards. The cross-sectional image was characterized by scanning electron microscopy (SEM, Hitachi S-4800). The XPS measurements were performed in a Kratos Ultra Spectrometer (a base pressure of 1×10^{-9} Torr) using monochromatized Al Kα X-ray photons (hυ=1486.6 eV) discharge lamp. UV-vis spectra were recorded using JASCO V-570 spectrophotometer. The film thickness was measured using an Ambios Technology XP-2 profilometer.

2.5 Carrier Mobility Extraction

The carrier saturation mobility μ in the investigated OTFTs calculated using the following equation [22]

$$I_{DS}=C_i\mu(W/2L)(V_{GS}-V_T)^2,$$

where I_{DS} is the drain current, C_i is the capacitance per unit area of the gate dielectric layer, W is the channel width, L is length, V_{GS} is the gate voltage, and V_T is threshold voltage.

RSC Advances Accepted Manuscript

This journal is © The Royal Society of Chemistry 2012

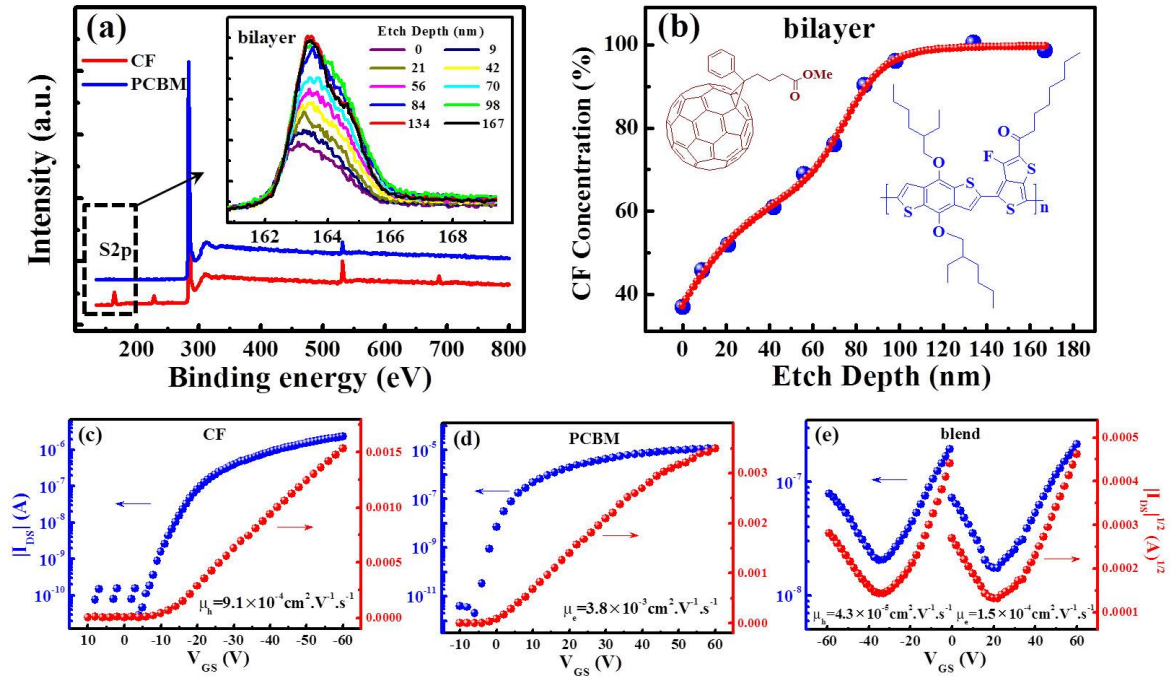

Figure 3. (a) The XPS spectra of the CF and PCBM. (b) Vertical composition profile from surface (deduced via etching and XPS characterization) for the bilayer film. Transfer curves of the OFETs: (c) for CF, (d) for PCBM and (e) CF:PCBM blend. The inset in (a) is the intensity of S 2p peak at different etch depth along the vertical direction from the surface.

3. Results and Discussion

The structure of the bilayer device and the molecular structures of CF and PCBM are given in **Figure 2a** and **2b**, respectively. The bilayer structure can be clearly seen in **Figure 2c,** which is the cross-sectional SEM of the bilayer film. For clarity we also marked the electrode, CF:PCBM blend and CF underlying layer in **Figure 2c**. The energy band diagrams of CF and PCBM are presented in **Figure 2d,** from which it can be concluded that the photo induced electrons will flow from CF into PCBM owing to the relative positions of their energy levels.[23,24] **Figure 1e** is a photograph of the fabricated devices on glass substrate.

In order to further confirm the bilayer structure, the concentration-depth profile of the bilayer film was studied by a widely used technique (slowly etching the prepared film from the surface accompanied by XPS measurement).[25] The chemical composition of the pristine CF and PCBM films were first analyzed via XPS in order to facilitate the calculation of the CF and PCBM composition in the bilayer film along the vertical direction from the surface. **Figure 3a** provides detailed information about the XPS test on the pristine CF and PCBM film spectra, and the intensity of S 2p peak at different etch depth along the vertical direction from the surface (S 2p peak located at 163.17 eV and regarded as the character peak for CF). By measuring the intensity of S 2p, the distribution of CF along the vertical direction from the surface can be calculated. The calculated CF concentration-depth profile of the bilayer film is presented in **Figure 3b**. For the bilayer film**,** the top ~100 nm from the surface is consisted of PCBM and CF, the concentration of CF then starts to increase from 38%, and reaches 100% when the depth from the surface reaches ~100 nm, and it remains unchanged with further increasing the depth (for this reason, we only etched 170 nm from the surface for the XPS measurement). The results give a strong evidence that our film is indeed bilayer structure: CF:PCBM blend (~100 nm)/CF (~400 nm).

For a photoconductor, it is well known that the photocurrent is closely related to responsivity (R) which is defined by the following equation:[26-29]

$$R = \frac{I_{Light} - I_{Dark}}{P_{ill}} = EQE\frac{\lambda q}{hc}G \qquad (1)$$

Where I_{Light} is current under the illumination, I_{Dark} is the dark current, P_{ill} is the incident illumination power on the effective area (channel area), *EQE* is the external quantum efficiency, λ is the wavelength of interest, *q* is the electron charge, *h* is the Planck constant and *c* is the speed of light. *G* is the photogain and defined as the ratio between the number of electrons collected per unit time and the number of absorbed photons per unit time, and can be expressed by the following equation:[28,29]

$$G = \frac{(\mu_n + \mu_p)\tau E}{L} \qquad (2)$$

RSC Advances Accepted Manuscript

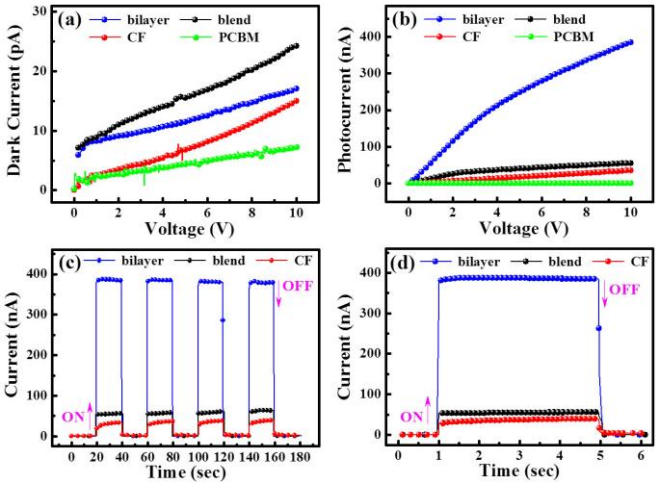

Figure 4. The performances of the fabricated devices based on the PCBM, CF, blend and bilayer films: (a) for I-V curves under dark; (b) for I-V curves under an incident white light density of 1.5 mWcm^{-2}; (c) and (d) are for the on/off switching properties (at a bias of 10V) under an incident white light density of 1.5 mWcm^{-2}.

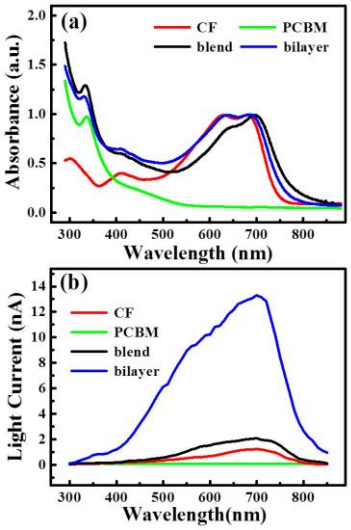

Figure 5. (a) Absorption spectra and (b) photocurrent spectra of the PCBM, CF, blend and bilayer films.

Where μ_n is the electron mobility, μ_p is the hole mobility, τ is the photo carrier lifetime, E is the electrical field and L is the device channel length.

From Equation (1) and (2), it is seen that photocurrent is proportional to carrier mobility μ, we thereby fabricated OFETs and extracted carrier mobilities in each films involved in this study (based on their transfer curves shown in **Figure 3c-e** and the Equation described in Experimental Section), which are listed here: hole mobilities in the CF film and the blend film are 9.1×10^{-4} and 4.3×10^{-5} cm^{2}V^{-1}s^{-1}, respectively. Electron mobilities in the PCBM film and the blend film are 3.8×10^{-3} and 1.5×10^{-4} cm^{2}V^{-1}s^{-1}, respectively. These mobility values are consistent with the reported ones.[16,30] It proved that hole/electron mobility is indeed decreased in the conventional blend film compared with pristine materials. We believe that in our bilayer device, by combining the efficient carrier generation in the blend layer (CF:PCBM) and relatively large hole mobility in the CF layer (in comparison to that in the blend film), the photocurrent can be improved.

In **Figure 4,** the performances of the fabricated photoconductors based on the PCBM, CF, blend and bilayer films are compared under dark and under an incident white light density of 1.5 mWcm^{-2}. The PCBM film shows very poor dark current and photocurrent (seen in **Figure 4a** and **Figure 4b**), and this should be induced by its large band gap (2.4 eV).[31] For the photocurrent: the CF film has much higher value compared with the PCBM film (seen in **Figure 4b**), which can be attributed to its much narrower band gap (1.7 eV). Because of the high exciton binding energy in conjugated polymers, thermal energy at room temperature is not sufficient to dissociate a photo exciton (typical with a binding energy of 0.4 eV) into free charge carriers.[10, 32] The free carriers that form the photocurrent in the PCBM and CF film should come from photo exciton dissociation induced by the external electric field and impurity inside the film.[33] The blend film shows slightly higher photocurrent in comparison to that of CF films (seen in **Figure 4b**). Considering that hole mobility in the blend film (4.3×10^{-5} cm^{2}V^{-1}s^{-1}) is actually lower than that in the CF film (9.1×10^{-4} cm^{2}V^{-1}s^{-1}), and electron mobility in the blend layer (1.5×10^{-4} cm^{2}V^{-1}s^{-1}) is also much lower than that in the PCBM film (3.8×10^{-3} cm^{2}V^{-1}s^{-1}), the photocurrent of the blend film obviously is induced by the greatly strengthened photo exciton dissociation, which produces much more free carriers.[8,9] The bilayer film exhibits significantly higher photocurrent than the PCBM film, the CF film and the blend film (seen in **Figure 4b**). This can be understood in the following way: photo excitons are firstly dissociated at the CF/PCBM interface in the blend layer, holes would diffuse from the CF in the blend layer into the CF layer (on bottom) because of the higher carrier concentrations in the blend layer, electrons then would stay in the blend layer (on top). Electrons then are transported in the blend layer and holes are transported in the CF layer between the two electrodes under a bias, and forms photocurrent. Since the CF layer has higher hole mobility than that in the blend film (9.1×10^{-4} vs 4.3×10^{-5} cm^{2}V^{-1}s^{-1}), thereby the photocurrent is enhanced (~7 times) in comparison to that of the blend film.

Figure 4c gives the on/off switching characteristics (at a bias of 10V) of the CF, blend and bilayer photoconductors, (No observable photocurrent was shown by the PCBM layer). The ON/OFF time duration is 20/20 seconds. It is clear seen that all these devices can be switched on and off repeatedly and the results are consistent with what is observed in **Figure 4b**. **Figure 4d** provides the light rise/decay information (at a bias of 10V) of the CF, blend and bilayer photoconductors, from which

RSC Advances Accepted Manuscript

This journal is © The Royal Society of Chemistry 2012

it can be calculated that the responses of all these devices are quite fast with rise/decay times shorter than 0.1/0.1 s.

The UV-Vis absorption spectra of the PCBM, CF, blend and bilayer films are given in **Figure 5a**. In the UV-Vis absorption spectra, broad absorption (from 300 to 800 nm) is seen for CF, while PCBM mainly shows light absorption in the UV region peaks at 347 nm. The absorptions of both the bilayer film and the blend film cover the ranges of both CF and PCBM. **Figure 5b** shows photocurrent as a function of wavelength for the PCBM, CF, blend and bilayer devices (under a bias of 10 V and an incident light density of 10.6 μWcm^{-2}). It is seen that across all the investigated wavelengths, photocurrent of the bilayer device is much higher than that of the PCBM, CF and blend devices, which should be an indication of the virtue of the bilayer architecture. Meanwhile, for all the three devices the spectral photocurrent matches well with the spectral absorption: stronger absorption always corresponds to larger photocurrent. This is in agreement with Equation (1): the photocurrent is linearly related to the EQE (EQE is linearly related to light absorption).

4. Conclusions

In summary, a solution processed bilayer architecture for OTFPs is demonstrated. In such bilayer OTFPs, free photo carriers are mainly generated in the top blend layer (CF:PCBM), holes in the blend layer then diffuse into the bottom CF layer, and electrons stay in the blend layer. The higher hole mobility in the CF layer (in comparison to that of the conventional blend film) leads to faster carrier transport, which in-turn results in better device performance. Principally, the all solution processed bilayer structure we designed here could pave a way for fabricating high-performance low-cost OTFPs in the future.

Acknowledgements

The authors acknowledge the financial support by 973 Program (Grant No. 2014CB643600 and 2011CB932304).

Notes and references

[1]*Beijing National Laboratory for Molecular Sciences, Key Laboratory of Organic Solids, Institute of Chemistry, Chinese Academy of Sciences, Beijing 100190, P.R. China E-mail: lihui@iccas.ac.cn, jizheng@iccas.ac.cn*

[2]*Department of Physics, Beijing Normal University, Beijing 100875, China*

[1] G. Dong; Y. Hu; C. Jiang; L. Wang and Y. Qiu, *Appl. Phys. Lett.*, 2006, **88**, 051110.

[2] J. Gao and F.A. Hegmann, *Appl. Phys. Lett.*, 2008, **93**, 223306.

[3] W. Woestenborghs; P. De Visschere; F. Beunis; G. Van Steenberge; K. Neyts and A. Vetsuypens, *Org. Electron.*, 2012, **13**, 2250-2256.

[4] N. Martino; D. Ghezzi; F. Benfenati; G. Lanzani and M.R. Antognazza, *J. Mater. Chem. B*, 2013, **1**, 3768-3780.

[5] Y. Zhang; T. Liu; B. Meng; X. Li; G. Liang; X. Hu and Q.J. Wang, *Nat. Commun.*, 2013, **4**, 1811.

[6] A. Iacchetti; D. Natali; M. Binda; L. Beverina and M. Sampietro, *Appl. Phys. Lett.*, 2012, **101**, 103307.

[7] J.W. Jeong; J.W. Huh; J.I. Lee; H.Y. Chu; J.J. Pak and B.K. Ju, *Thin Solid Films*, 2010, **518**, 6343-6347.

[8] G. Yu; J. Gao; J. Hummelen; F. Wudl and A. Heeger, *Science*, 1995, **270**, 1789-1790.

[9] T. Erb; U. Zhokhavets; G. Gobsch; S. Raleva; B. Stühn; P. Schilinsky; C. Waldauf and C.J. Brabec, *Adv. Funct. Mater.*, 2005, **15**, 1193-1196.

[10]P.W. Blom; V.D. Mihailetchi; L.J.A. Koster and D.E. Markov, *Adv. Mater.*, 2007, **19**, 1551-1566.

[11]J. Peet; C. Soci; R.C. Coffin; T.Q. Nguyen; A. Mikhailovsky; D. Moses and G.C. Bazan, *Appl. Phys. Lett.*, 2006, **89**, 252105.

[12]M.M. Wienk; J.M. Kroon; W.J.H. Verhees; J. Knol; J.C. Hummelen; P.A. van Hal and R.A.J. Janssen, *Angew. Chem.*, 2003, **115**, 3493-3497.

[13]H.-C. Liao; C.-P. Hsu; M.-C. Wu; C.-F. Lu and W.-F. Su, *Anal. Chem.*, 2013, **85**, 9305-9311.

[14]S.-M. Li; D.-J. Xue; W. Xu; Y. Feng; J. Wang; G. Zhang; X. Meng; C.-R. Wang; Y. Song and C.-Y. Shu, *J. Mater. Chem.C.*, 2014, **2**, 1500-1504.

[15]S. Günes; H. Neugebauer and N.S. Sariciftci, *Chem. Rev.*, 2007, **107**, 1324-1338.

[16]E. Von Hauff; V. Dyakonov and J. Parisi, *Sol. Energy Mater. Sol. Cells*, 2005, **87**, 149-156.

[17]Z. Jin and J. Wang, *Appl. Phys. Lett.*, 2013, **102**, 053304.

[18]Z. Jin and J. Wang, *J. Mater. Chem.C.*, 2013, **1**, 7996-8002.

[19]M. Granström; K. Petritsch; A. Arias; A. Lux; M. Andersson and R. Friend, *Nature*, 1998, **395**, 257-260.

[20]A.L. Ayzner; C.J. Tassone; S.H. Tolbert and B.J. Schwartz, *J.Phys.Chem.C.*, 2009, **113**, 20050-20060.

[21]G. Dennler; H.-J. Prall; R. Koeppe; M. Egginger; R. Autengruber and N.S. Sariciftci, *Appl. Phys. Lett.*, 2006, **89**, 073502.

[22]Z. Jin and J. Wang, *J. Mater. Chem.C.*, 2014, **2**, 1966-1970.

[23]H.-Y. Chen; J. Hou; S. Zhang; Y. Liang; G. Yang; Y. Yang; L. Yu; Y. Wu and G. Li, *Nat. Photonics*, 2009, **3**, 649-653.

[24]J.Y. Kim; S.H. Kim; H.H. Lee; K. Lee; W. Ma; X. Gong and A.J. Heeger, *Adv. Mater.*, 2006, **18**, 572-576.

[25]T. Hori; A. Semba; S. Lee; H. Kubo; A. Fujii and M. Ozaki, *Thin Solid Films*, 2014, **554**, 222-225.

[26]M.K. Jana; P. Chithaiah; B. Murali; S.B. Krupanidhi; K. Biswas and C.N.R. Rao, *J. Mater. Chem.C.*, 2013, **1**, 6184-6187.

[27]Y. Zhou; L. Wang; J. Wang; J. Pei and Y. Cao, *Adv. Mater.*, 2008, **20**, 3745-3749.

[28]S.M. Sze and K.K. Ng, *Physics of semiconductor devices*. 2nd ed.; Wiley: New York, 2006; p 667-671.

[29]Z. Jin; L. Gao; Q. Zhou and J. Wang, *Sci. Rep.*, 2014, **4**, 4268.

[30]L. Huo; S. Zhang; X. Guo; F. Xu; Y. Li and J. Hou, *Angew. Chem.*, 2011, **123**, 9871-9876.

[31]J. Schafferhans; A. Baumann; A. Wagenpfahl; C. Deibel and V. Dyakonov, *Org. Electron.*, 2010, **11**, 1693-1700.

[32]Z. Jin and J. Wang, *Sci. Rep.*, 2014, **4**, 5331.

[33]M.C. Hamilton; S. Martin and J. Kanicki, *IEEE T. Electron Dev.*, 2004, **51**, 877-885.

RSC Advances Accepted Manuscript